

In Vitro Autoradiographic Localization of ¹²⁵I-Secretin Receptor Binding Sites in Rat Brain

Satoshi Nozaki,* Rika Nakata,† Hiroshi Mizuma,† Nobuhiro Nishimura,† Yumiko Watanabe,* Ryuichiro Kohashi,† and Yasuyoshi Watanabe*¹

*Department of Physiology, Osaka City University Graduate School of Medicine, 1-4-3 Asahimachi, Abeno-ku, Osaka 545-8585, Japan; and †Department of Clinical Pathology, School of Health Sciences, Kyorin University, 476 Miyashita-cho, Hachioji, Tokyo 192-8508, Japan

Received February 11, 2002

Although the existence of the receptor for secretin in the brain was suggested, the localization of secretin receptor and the neuronal function of secretin have not been clarified yet. In the present study, the localization of secretin receptor was investigated in the rat brain by using an *in vitro* autoradiography technique. Frozen section autoradiography with ¹²⁵I-secretin showed intense binding in the nucleus of solitary tract, laterodorsal thalamic nucleus, and accumbens nucleus; moderate binding in the hippocampus, caudate/putamen, cerebellum, cingulate and orbital cortices. Scatchard plot analysis gave the K_d value of 125 pM with B_{max} of 134 fmol/mg tissue in the hippocampus. The binding specificity was confirmed with secretin and its analogs, VIP, PACAP, and glucagon. These results indicate the secretin receptor system might have some neural functions in the brain, which could give the basis for therapeutic use of secretin in autistic children. © 2002 Elsevier Science (USA)

Key Words: secretin; receptor; *in vitro*; autoradiography; brain; localization.

In 1998, in the course of the treatment for digestive function of the patients with autism, the dramatic effect of secretin was reported in the social behavior of autistic children (1). Secretin is a 27-amino acid neuroendocrine peptide that is a member of the VIP, PACAP, and glucagon peptide family. It is produced by the endocrine S cells, which are localized in the mucosa of proximal small intestine (2). The primary action of secretin is to stimulate bicarbonate, electrolyte and volume secretion from pancreatic ductile epithelial cells (3). Secretin-like immunoreactivity or bioactivity was reported to have been detected in the brain.

¹ To whom correspondence should be addressed. Fax: +81-6-6645-3712. E-mail: yywata@med.osaka-cu.ac.jp.

O'Donohue *et al.* (4) reported that secretin-like immunoreactivity is widely distributed in the brain and the levels of immunoreactivity in the brain were higher than or comparable to those in the duodenum. Moreover, the secretin precursor gene was widely expressed in the brain and hypophysis (5). The function of secretin is mediated via its specific interaction with cell surface receptor(s) (6). The existence of the receptor for secretin in the brain was suggested (7), and in cultured neurons and neuroblastoma × glioma hybrid cells, secretin stimulates adenylate cyclase as a second messenger (8). Furthermore, in rat superior cervical ganglion neurons and PC-12 cells, secretin activates tyrosine hydroxylase activity (9, 10). However, the localization of secretin receptor and the neuronal function of secretin have not been clarified yet. We here report the localization of secretin receptor by *in vitro* autoradiography in rat brain.

MATERIALS AND METHODS

Materials. ¹²⁵I-Secretin (porcine) was purchased from Peninsula Laboratories, Inc. (CA, USA). The specific radioactivity was 2000 Ci/mmol (74 kBq/mmol). Secretin (porcine), Vasoactive Intestinal Peptide (VIP) (human, porcine), and Pituitary Adenylate Cyclase Activating Polypeptide fragment 38 (PACAP38) (human, ovine, rat) were purchased from Peptide Institute Inc. (Osaka, Japan). Glucagon (human, ovine, porcine) was purchased from Sigma-Aldrich. Autoradiographic ¹²⁵I-microscales were purchased from Amersham Pharmacia Biotech. Imaging plates (BAS MS2040) for imaging analyzer (BAS2500) were purchased from Fuji Film Co. (Tokyo, Japan).

Animals. The Animal Ethics Committee of Osaka City University Graduate School of Medicine approved all experiments with research animals. Male 5- to 6-week-old Sprague-Dawley rats (Japan SLC Co., Hamamatsu), weighing 160–180 g, were used. The animals were housed with free access to standard laboratory chow in an air-conditioned room under a constant 12-h light and dark cycle (lights on at 8:00 a.m.) at a temperature of 22–24°C and 60–70% relative humidity.

In vitro receptor autoradiography. The rats were anesthetized with diethyl ether and perfused via the left ventricle with ice-cold 10

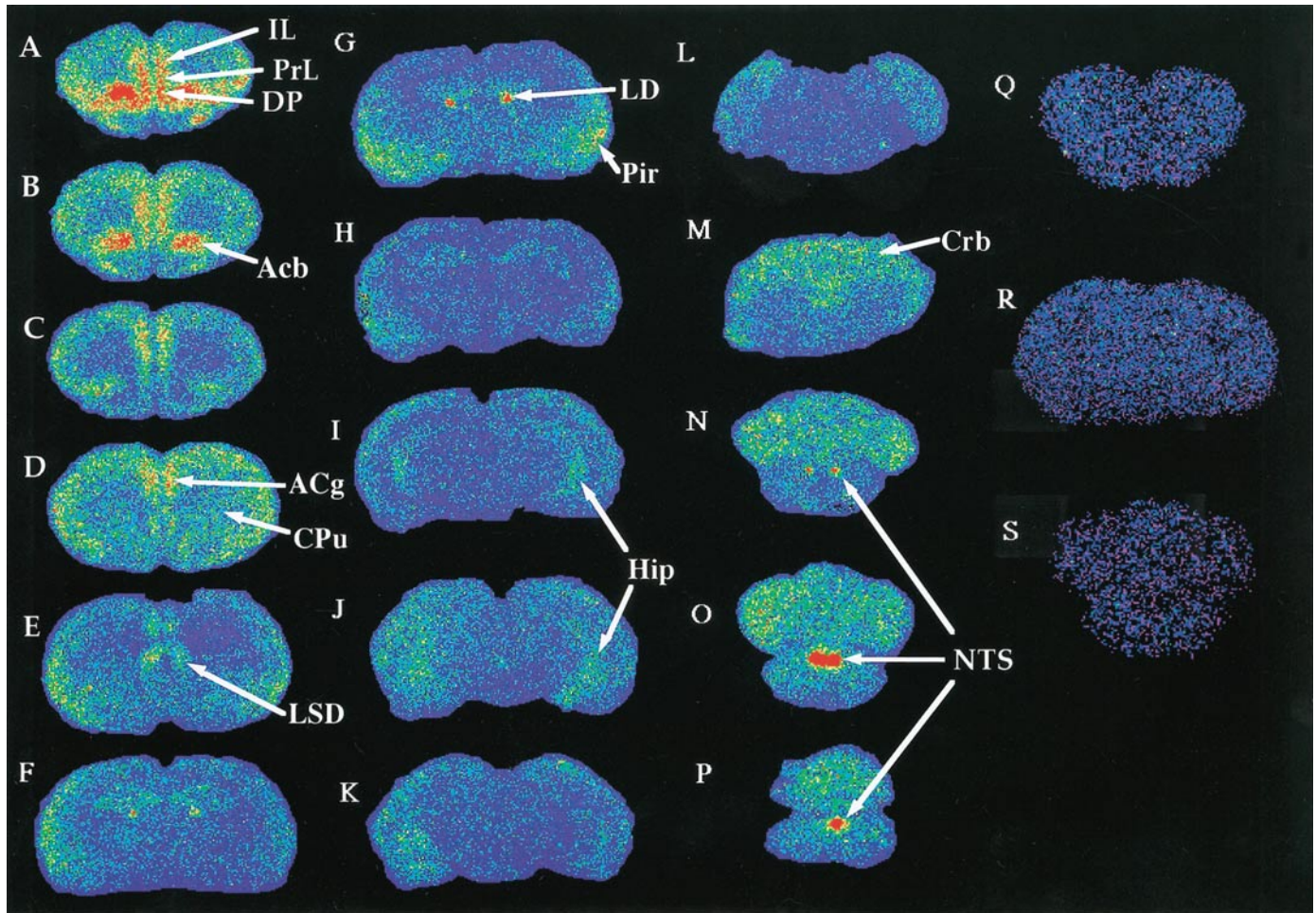


FIG. 1. *In vitro* autoradiographic localization of the ^{125}I -secretin binding sites in rat brain. (A–P) Pseudo-color coding images of total binding in representative brain regions. (Q–S) Pseudo-color coding images of nonspecific binding in the presence of $1\ \mu\text{M}$ unlabeled secretin. The same color coding scale in A–S was used. Q, R, and S were adjacent sections of A, G, and O, respectively. Cryostat sections were incubated with $50\ \text{pM}$ ^{125}I -secretin at 20°C for 90 min, washed, air-dried, and exposed to the imaging plate. The data were obtained as described under Materials and Methods. PrL, prelimbic cortex; IL, infralimbic cortex; DP, dorsal peduncular cortex; Acb, nucleus accumbens; ACg, anterior cingulate; LSD, lateral septal nucleus dorsalis; LD, laterodorsal thalamic nucleus; CPu, caudate putamen; Pir, piriform cortex; Hip, hippocampus; Crb, cerebellum; NTS, nucleus of solitary tract.

mM sodium phosphate-buffered saline (pH 7.4). The brain was rapidly removed, and was frozen in dry-ice powder. Frozen serial sections of $10\ \mu\text{m}$ thickness were cut in a cryostat at -17°C and mounted on 3-Amino-Propyltriethoxy Silane (APS)-coated glass slides. The sections were preincubated at 20°C , twice for 10 min in $50\ \text{mM}$ Tris-HCl buffer (pH 7.4) containing 0.5% bovine serum albumin. The incubation was then performed in the same buffer but further containing $5\ \text{mM}$ MgCl_2 , 0.05% bacitracin, $2\ \text{mM}$ EGTA, and $50\ \text{pM}$ of ^{125}I -secretin (porcine) at 20°C for 90 min. Then the slides were washed twice for 10 min in ice-cold preincubation buffer but containing $5\ \text{mM}$ MgCl_2 , then dipped in $50\ \text{mM}$ Tris-HCl buffer (pH 7.4) containing $5\ \text{mM}$ MgCl_2 , and air dried. Nonspecific binding was determined in the presence of unlabeled $1\ \mu\text{M}$ secretin. After having been dried in a desiccator, the slides were exposed to the imaging plate (BAS MS2040).

Image analysis and quantification. The autoradiograms were quantified with a Bio-Image Analyzer BAS2500 (Fuji Photo Film Co., Ltd., Tokyo, Japan). After calibration with autoradiographic ^{125}I -microscales (RPA523, Amersham Pharmacia Biotech, UK), quanti-

tative analysis was performed with NIH image analysis software (11).

Scatchard plot analysis. The values of saturable specific ^{125}I -secretin (10 – $80\ \text{pM}$) binding were transformed into the Scatchard plot. For evaluation of binding data, the curve-fitting analysis program CA-Cricket Graph III (Computer Associates International Inc.) was used.

RESULTS

As shown in Fig. 1 and Table 1, the highest binding was observed in the nucleus of solitary tract ($74.2 \pm 6.9\ \text{fmol/mg}$ tissue), followed by that in the laterodorsal thalamic nucleus ($55.7 \pm 6.4\ \text{fmol/mg}$ tissue) and accumbens nucleus ($36.5 \pm 1.4\ \text{fmol/mg}$ tissue). In the cortical regions, the binding was moderate in the orbital, cingulate, piriform, frontal, parietal and entorhi-

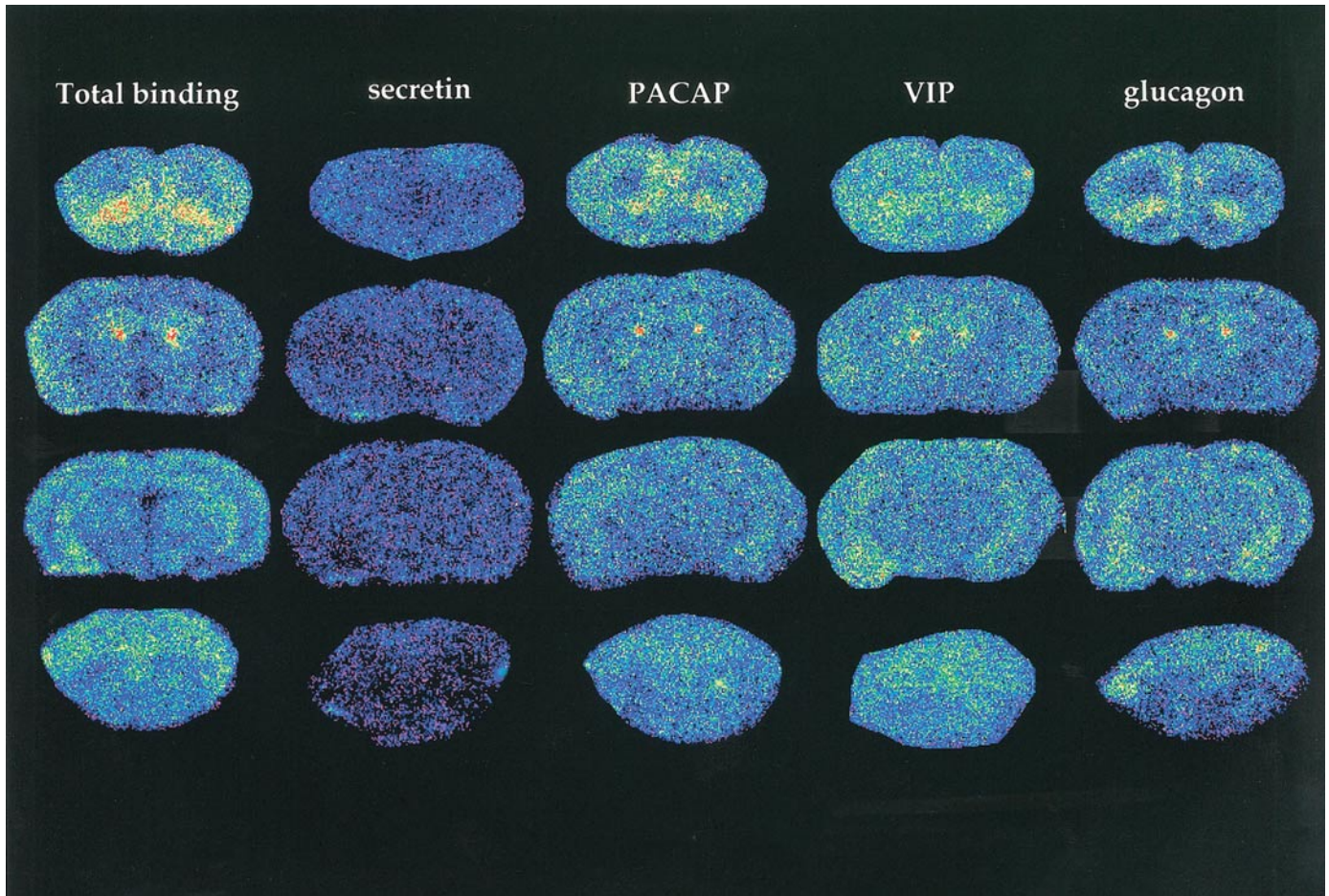


FIG. 2. Displacement of ^{125}I -secretin binding by secretin, PACAP. Unlabeled peptides, secretin, PACAP, VIP, and glucagons, were added to the binding buffer. The displacement of ^{125}I -secretin binding in the accumbens nucleus, laterodorsal thalamic nucleus, hippocampus, and cerebellum were shown. Total binding with 50 pM ^{125}I -secretin (Total binding) was displaced almost completely with unlabeled 100 nM secretin (secretin), but very slightly with 100 nM PACAP (PACAP), 100 nM VIP (VIP), or 100 nM glucagon (glucagon).

nal cortices. Moderate binding was also seen in the caudate/putamen, hippocampus, lateral septal nucleus, olfactory bulb, amygdala, hypothalamus, pineal body, pituitary gland, dorsal Raphe nucleus, locus coeruleus, and cerebellum. The binding was low in the corpus callosum.

To study the specificity of secretin receptor binding, we employed the peptides of VIP family, namely, VIP, PACAP, and glucagon. Figure 2 shows displacement of 50 pM ^{125}I -secretin binding with 100 nM secretin, PACAP, VIP, and glucagons in the consecutive sections including the accumbens nucleus, laterodorsal thalamic nucleus, hippocampus, and cerebellum as representative regions. In all these regions and other brain regions, ^{125}I -secretin binding was completely displaced by 100 nM secretin. However, ^{125}I -secretin binding was hardly displaced by the same concentration of secretin analogs (PACAP, VIP, and glucagon).

To further characterize secretin receptor binding, we performed Scatchard plot analysis. As shown in Fig. 3,

there was a single component of binding with K_d and B_{max} values being 125 pM and 134 fmol/mg tissue, respectively, in the hippocampus.

DISCUSSION

The previous report with ^{125}I -secretin suggested the existence of secretin receptor in membrane fractions of rat brain (7). As far as we know, our present result is the first report demonstrating the autoradiographic localization of secretin binding sites in the brain. The localization of VIP receptor was shown by Vertongen *et al.* (12), which is dense in the superior colliculus, ventral posterior thalamic nucleus, dorsal raphe nucleus, dentate gyrus, suprachiasmatic nucleus, supraoptic nucleus, accumbens nucleus. On the other hand, the PACAP receptor was enriched in the piriform cortex, diagonal band, accumbens nucleus, caudate/putamen, hippocampus, habenular nucleus, lateral hypothalamic nucleus, superior colliculus, dorsal raphe nu-

cleus (13). Thus, in the rat brain, the localization of secretin, VIP, and PACAP binding sites showed different patterns, indicating the presence of the receptors specific for each peptide. The data from the displacement study with unlabelled peptides on ¹²⁵I-secretin binding sites, as shown in Fig. 2, confirmed the idea.

Previously, Couvineau *et al.* (14) showed that secretin weakly competes with VIP for the VIP receptor purified from porcine liver. Their results suggest that secretin and VIP receptors are structurally related, and it might be possible that VIP, PACAP and glucagon could weakly compete with ¹²⁵I-secretin binding, in a sense of low-affinity binding sites.

Furthermore, on the basis of the Scatchard plot analysis, the K_d and B_{max} values for ¹²⁵I-secretin binding sites showed high affinity (125 pM) and medium density (134 fmol/mg tissue) in the hippocampus. Previously, Fremeau *et al.* (7) reported that the binding of ¹²⁵I-secretin to rat brain membranes was specific, saturable, and reversible, and that the binding has high affinity (K_d = 0.2 nM) to a single class of noninteracting sites. These results strongly indicate that the receptor specific for secretin exists in rat brain, and it

TABLE 1
Regional Distribution of ¹²⁵I-Secretin Binding in Rat Brain

Brain regions	fmol/mg tissue	SEM
Olfactory bulb	16.3	±1.3
Lateral septal nucleus, intermediate	15.3	±1.8
Lateral septal nucleus, dorsal	20.5	±1.5
Accumbens nucleus	36.5	±1.3
Caudate putamen, posterior	20.2	±1.1
Caudate putamen, anterior	12.1	±1.0
Amygdala	15.8	±0.8
Corpus callosum	6.3	±1.0
Cortex		
Orbital	24.7	±1.8
Frontal	17.3	±3.1
Cingulate	22.0	±0.9
Piriform	18.8	±0.7
Parietal	16.4	±1.2
Entorhinal	16.0	±0.6
Thalamus	16.1	±1.0
Laterodorsal thalamic nucleus	55.7	±6.3
Hypothalamus	14.7	±0.9
Hippocampus	22.5	±0.8
Pituitary gland	15.9	±5.7
Pineal body	13.1	±1.7
Dosal raphe nucleus	14.0	±1.9
Locus coeruleus	10.0	±0.7
Nucleus of solitary tract	74.2	±6.9
Cerebellum	23.7	±0.6

Note. Frozen sections from rat brains were incubated with 50 pM ¹²⁵I-secretin in the presence or absence of 1 μM secretin. After autoradiography with ¹²⁵I-labeled microscases, images were analyzed quantitatively as described under Materials and Methods. The values were the means ± standard errors of four brains obtained from the same structure on contiguous sections.

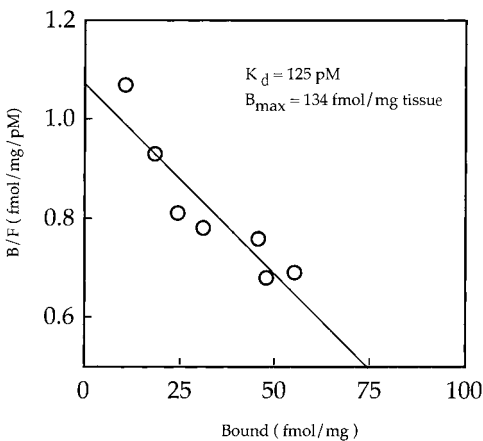


FIG. 3. Scatchard plot analysis of ¹²⁵I-secretin binding. The values of saturable specific ¹²⁵I-secretin binding were transformed into the Scatchard plot. The line shows the fitted curve with CA-Cricket graph. The data resulted in assignment of affinity constant (K_d), and binding site density (B_{max}).

may play some roles in the brain function. Our results give a basis for further study on the neural function of secretin, and therefore in the future extend to explain therapeutic effect of secretin on the autistic children.

ACKNOWLEDGMENTS

This study was supported in part by Research for the Future Program (RFTF) JSPS-RFTF 98L00201 from the Japan Society for the Promotion of Science (JSPS), by a Grant-in-Aid for Scientific Research on Priority Areas (C)-Advanced Brain Science Project from the Ministry of Education, Culture, Science, Sports and Technology of Japan to Y.W. (13210120), and by Project Research Grants of Kyorin University to R.K. (00-03-03).

REFERENCES

1. Horvath, K., Stefanatos, G., Sokolski, K. N., Wachtel, R., Nabors, L., and Tildon, J. T. (1998) Improved social and language skills after secretin administration in patients with autistic spectrum disorders. *J. Assoc. Acad. Minor. Phys.* **9**, 9–15.
2. Chey, W. Y., and Chang, T. (1989) in *Handbook of Physiology* (Raunar, B. B., Ed.), Vol. 2, Section 6, pp. 359–402, American Physiological Society, Bethesda, MD.
3. Bayliss, W. M., and Starling, E. H. (1902) The mechanism of pancreatic secretion. *J. Physiol.* **28**, 325–353.
4. O'Donohue, T. L., Charlton, C. G., Miller, R. L., Boden, G., and Jacobowitz, D. M. (1981) Identification, characterization, and distribution of secretin immunoreactivity in rat and pig brain. *Proc. Natl. Acad. Sci. U.S.A.* **78**, 5221–5224.
5. Itoh, N., Furuya, T., Ozaki, K., Ohta, M., and Kawasaki, T. (1991) The secretin precursor gene: Structure of the coding region and expression in the brain. *J. Biol. Chem.* **266**, 12595–12598.
6. Jensen, R. T., Charlton, C. G., Adachi, H., Jones, S. W., O'Donohue, T. L., and Gardner, J. D. (1983) Use of ¹²⁵I-secretin to identify and characterize high-affinity secretin receptors on pancreatic acini. *Am. J. Physiol.* **245**, G186–195.
7. Fremeau, R. T., Jr., Jensen, R. T., Charlton, C. G., Miller, R. L.,

- O'Donohue, T. L., and Moody, T. W. (1983) Secretin: Specific binding to rat brain membranes. *J. Neurosci.* **3**, 1620–1625.
8. Roth, B. L., Beinfeld, M. C., and Howlett, A. C. (1984) Secretin receptors on neuroblastoma cell membranes: Characterization of ¹²⁵I-labeled secretin binding and association with adenylate cyclase. *J. Neurochem.* **42**, 1145–1152.
9. Ip, N. Y., Baldwin, C., and Zigmond, R. E. (1985) Regulation of the concentration of adenosine 3',5'-cyclic monophosphate and the activity of tyrosine hydroxylase in the rat superior cervical ganglion by three neuropeptides of the secretin family. *J. Neurosci.* **5**, 1947–1954.
10. Roskoski, R., Jr., White, L., Knowlton, R., and Roskoski, L. M. (1989) Regulation of tyrosine hydroxylase activity in rat PC12 cells by neuropeptides of the secretin family. *Mol. Pharmacol.* **36**, 925–931.
11. Lennard, P. R. (1990) Image analysis for all. *Nature* **347**, 103–104.
12. Vertongen, P., Schiffmann, S. N., Gourlet, P., and Robberecht, P. (1998) Autoradiographic visualization of the receptor subclasses for vasoactive intestinal polypeptide (VIP) in rat brain. *Ann. N.Y. Acad. Sci.* **11**, 412–415.
13. Masuo, Y., Ohtaki, T., Masuda, Y., Tsuda, M., and Fujino, M. (1992) Binding sites for pituitary adenylate cyclase activating polypeptide (PACAP): Comparison with vasoactive intestinal polypeptide (VIP) binding site localization in rat brain sections. *Brain Res.* **575**, 113–123.
14. Couvineau, A., Voisin, T., Guijarro, L., and Laburthe, M. (1990) Purification of vasoactive intestinal peptide receptor from porcine liver by a newly designed one-step affinity chromatography. *J. Biol. Chem.* **265**, 13386–13390.